The conserved phosphatase GSP-2/PP1 promotes germline immortality via small RNA-mediated genome silencing during meiosis

Katherine Kretovich Billmyre[1,2], Anna-Lisa Doebley[2,7,8], Bree Heestand[1,2], Tony Belicard[3,4], Aya Sato-Carlton[5], Stephane Flibotte[6], Matt Simon[1,2,9], Megan Gnazzo[7], Ahna Skop[7], Donald Moerman[6], Peter Mark Carlton[5], Peter Sarkies[3,4] and Shawn Ahmed[1,2]

[1]Department of Genetics, University of North Carolina, Chapel Hill, NC, 27599 USA
[2]Department of Biology, University of North Carolina, Chapel Hill, NC, 27599 USA
[3]Medical Research Council London Institute of Medical Sciences, Du Cane Road, London, W12 0NN, UK
[4]Institute for Clinical Sciences, Imperial College London, Du Cane Road, London, W12 0NN, UK
[5]Graduate school of Biostudies, Kyoto University, Kyoto, 606-8501, Japan,
[6]Department of Zoology, University of British Columbia, Vancouver, British Columbia, Canada
[7]Department of Genetics, University of Wisconsin-Madison, Madison, WI 53706
[8]Present address: Department of Opthamology, University of Washington, Seattle, WA, USA
[9]Present address: Department of Biology, University of Rochester, Rochester, NY, USA

*To whom correspondence should be addressed. E-mail: shawn@med.unc.edu

Abstract

Genomic silencing can promote germ cell immortality, or transgenerational maintenance of the germ line, via mechanisms that may occur during mitosis or meiosis. Here we report that the *gsp-2* PP1/Glc7 phosphatase promotes germ cell immortality. We identified a separation-of-function allele of *C. elegans* GSP-2 that caused a meiosis-specific chromosome segregation defect and defects in transgenerational small RNA-induced genome silencing. GSP-2 is recruited to meiotic chromosomes by LAB-1, which also promoted germ cell immortality. Sterile *gsp-2* and *lab-1* mutant adults displayed germline degeneration, univalents and histone phosphorylation defects in oocytes, similar to small RNA genome silencing mutants. Epistasis and RNA analysis suggested that GSP-2 functions downstream of small RNAs. We conclude that a meiosis-specific function of GSP-2/LAB-1 ties small RNA-mediated silencing of the epigenome to germ cell immortality. Given that hemizygous genetic elements can drive transgenerational epigenomic silencing, and given that LAB-1 promotes pairing of homologous chromosomes and localizes to the interface between homologous chromosomes during pachytene, we suggest that discontinuities at this interface could promote nuclear silencing in a manner that depends on GSP-2.

Author Summary

The germ line of an organism is considered immortal in its capacity to give rise to an unlimited number of future generations. To protect the integrity of the germ line, mechanisms act to suppress the accumulation of transgenerational damage to the genome or epigenome. Loss of germ cell immortality can result from mutations that

disrupt the small RNA-mediated silencing pathway that helps to protect the integrity of the epigenome. Here we report for the first time that the *C. elegans* protein phosphatase GSP-2 that promotes core chromosome biology functions during meiosis is also required for germ cell immortality. Specifically, we identified a partial loss of function allele of *gsp-2* that exhibits defects in meiotic chromosome segregation and is also dysfunctional for transgenerational small RNA-mediated genome silencing. Our results are consistent with a known role of *Drosophila* Protein Phosphatase 1 in heterochromatin silencing, and point to a meiotic phosphatase function that is relevant to germ cell immortality, conceivably related to its roles in chromosome pairing or sister chromatid cohesion.

Introduction

Animals, including humans, are comprised of two broad cell types: somatic cells and germ cells. Somatic cells consist of many diverse differentiated cell types, while germ cells are specialized to produce the next generation of offspring. An important difference between these two cell types is that somatic cells undergo aging phenomena while the germ line is effectively immortal and capable of creating new “young” offspring [1]. Understanding the basis of immortality in germ cells may provide insight into why organisms age.

In *C. elegans*, disruption of pathways that promote germ cell immortality results in initially fertile animals that become sterile after reproduction for a number of generations. Many such *mortal germline* (*mrt*) mutant strains are temperature-sensitive, becoming sterile at 25°C but remaining fertile indefinitely at 20°C [2]. Mutations that

cause a Mrt phenotype have been reported in two distinct pathways: telomerase-mediated telomere maintenance [3,4] and small RNA-mediated nuclear silencing [5–9]. Mutations in the PIWI Argonaute protein cause immediate sterility in many species. However, disruption of the *C. elegans* Piwi orthologue PRG-1, which interacts with thousands of piRNAs to promote silencing of some genes and many transposons in germ cells, results in temperature-sensitive reductions in fertility and in an unconditional Mrt phenotype [6–12]. Multiple members of a nuclear RNA interference (RNAi) pathway that promotes maintenance of transgene silencing also promote germ cell immortality and likely function downstream of PRG-1/piRNAs [10,13]. One nuclear RNAi defective mutant, *nrde-2,* a number of heritable RNAi mutants, including *hrde-1*, and two RNAi defective mutants, *rsd-2* and *rsd-6*, only become sterile after growth for multiple generations at the restrictive temperature of 25°C [10,12–16]. These 'small RNA-mediated genome silencing' genes repress deleterious genomic elements via a small RNA-mediated memory of 'self' vs 'non-self' segments of the genome [13,17,18]. The transgenerational fertility defects of such mutants could reflect a progressive desilencing of heterochromatin due to changes in histone modifications downstream of small RNAs, which is modulated by histone modifications that occur in response to small RNAs, such as H3K4 demethylation and H3K9me2/3 [15,19].

Pioneering studies in *Neurospora* demonstrated that unsuccessful pairing of DNA during meiotic prophase can trigger small RNA-mediated genome silencing [20], and multigenerational silencing of hemizygous transgenes [21] suggests similar mechanisms may operate in *C. elegans*. Components of the *C. elegans* small RNA-mediated genome silencing machinery, such as the HRDE-1 and PRG-1 Argonaute

proteins, are expressed throughout germ cell development [6,10,13,18]. RSD-2 displays a cytoplasmic localization in embryos but becomes a nuclear protein in adults [12], suggesting that aspects of small RNA-mediated genome silencing may be developmentally plastic.

Here we report the identification of a hypomorphic allele of *gsp-2*, a PP1/Glc7 phosphatase, which fails to maintain germline immortality at 25°C. GSP-2 is one of four PP1 catalytic subunits in *C. elegans* [22,23]. The PP1 phosphatase has roles in many cellular processes including mitosis, meiosis, apoptosis and protein synthesis [24]. Previously, GSP-2 has been shown to promote meiotic chromosome cohesion by restricting the activity of the Aurora B kinase ortholog AIR-2 to the short arms of *C. elegans* chromosomes during Meiosis I [25,26]. Here, we demonstrate that GSP-2 promotes germline immortality via a small RNA-mediated genome silencing pathway, implicating pairing and/or cohesion of meiotic chromosomes in genomic silencing.

Results

Identification of GSP-2 as a temperature-sensitive *mrt* mutant

In a screen for *mrt* mutants [2], one mutation that displayed a Temperature-sensitive defect in germ cell immortality, *yp14*, was tightly linked to an X chromosome segregation defect manifesting as a High Incidence of Males (Him) phenotype, such that 3.9% of *yp14* self-progeny were XO males, which significantly greater than the 0.05% male self-progeny observed in wildtype animals (Fig. 1A, p<.0001). The *yp14* mutation was mapped to Chromosome *III*, and whole genome sequencing revealed missense mutations in 6 genes within the *yp14* interval (Fig. S1A,B). Three-factor

mapping of the *yp14* Him and Mrt phenotypes suggested that *yp14* might correspond to the missense mutation in *gsp-2* (Fig. 1C,D) or to a mutation in the G-protein coupled receptor gene *srb-11* (Fig. S1A,B).

To test whether the meiotic segregation phenotype of *yp14* was due to a mutation in *gsp-2*, we performed a non-complementation test with a deletion mutation in *gsp-2*, *tm301*. *yp14* / *tm301* F1 heterozygous hermaphrodites gave rise to F2 male progeny at a frequency of 5.7% at 20°C, similar to the 3.8% male phenotype observed for *yp14* homozygotes (Fig. S1C). Thus, *tm301* failed to complement *gsp-2(yp14)* for its Him phenotype. In contrast, *gsp-2(tm301)* / + animals did not display a Him phenotype (Fig. S1C). *gsp-2(yp14)* strains also displayed 6% embryonic lethality at 20°C (Fig. 1B). Given that most forms of aneuploidy for the five *C. elegans* autosomes elicit embryonic lethality [27], the simplest explanation for the Him and Embryonic Lethal phenotypes of *gsp-2(yp14)* is that they are due to chromosome mis-segregation. Both of these phenotypes were exacerbated at 25°C (Fig. 1A,B), suggesting that *gsp-2(yp14)* has a chromosome segregation defect that may be mechanistically linked to its Mortal Germline phenotype (Fig. 1A,E). At both temperatures, the X chromosome non-disjunction defect was more pronounced than the embryonic lethality associated with non-disjunction of any of the five *C. elegans* autosomes (Table S1).

gsp-2(tm301) null mutants immediately exhibited high levels of embryonic lethality at 20°C with a few F3 embryos that survive until adulthood (Fig. 1C), consistent with roles for PP1 in chromosome condensation and segregation during mitosis in several species [28–30]. Mutations that cause chromosome non-disjunction during mitosis occasionally lead to loss of an X chromosome during germ cell development,

154 which could result in the stochastic appearance of XX hermaphrodites with high
155 numbers of XO male progeny [27]. However, jackpots of XO males did not occur when
156 *yp14* mutant hermaphrodites were isolated as single L4 larvae (Fig. 1G), implying that
157 *yp14* is a separation-of-function mutation that specifically compromises the meiotic
158 chromosome segregation function of GSP-2 without affecting its function in mitosis.
159
160 **GSP-2 promotes germline immortality at high temperature**
161 GSP-2 is assumed to be localized to the long arms of meiotic chromosomes
162 through binding to LAB-1, where it antagonizes AIR-2 (Aurora-B kinase) activity to
163 regulate cohesion during meiotic prophase and Meiosis I [26,28,30]. In addition, LAB-1
164 is also present on mitotic chromosomes where it likely antagonizes AIR-2 activity [25].
165 In meiosis, LAB-1 fulfills the roles played by Shugoshin and Protein Phosphatase 2A in
166 many other organisms, by protecting meiotic chromosome cohesion on the long arms in
167 Meiosis I [25,31,32]. Once recruited by LAB-1, GSP-2 keeps REC-8, a meiosis-specific
168 cohesin subunit, dephosphorylated to protect it from premature degradation and
169 chromatid separation [25,26].
170 At 20°C, *gsp-2(yp14)* mutants remain fertile indefinitely, but at 25°C they exhibit
171 sterility between generations F5 and F17 (Fig. 1E,F). We asked if a meiotic function of
172 GSP-2 is relevant to germ cell immortality by first outcrossing a *lab-1* deletion with
173 wildtype and re-isolating *lab-1* homozygotes in an effort to eliminate epigenetic defects
174 that could have accumulated in the parental *lab-1* strain. Outcrossed *lab-1* mutants
175 displayed a Mortal Germline phenotype at 25°C (Fig. 1E,F). We created *lab-1;gsp-2*
176 double mutants, which remained fertile indefinitely when grown at 20°C but displayed a

177 slightly accelerated number of generations to sterility at 25°C in comparison with *lab-1*
178 mutants (Fig. 1E,F). Together, these results suggest that a meiotic function of GSP-2
179 that is directed by LAB-1 promotes germ cell immortality. Moreover, the weak Mortal
180 Germline phenotype of *lab-1* single mutants at 20°C was suppressed by *gsp-2(yp14)*
181 (Log Rank Test, p=.001).
182
183 **_gsp-2_ and _lab-1_ mutants display common germline defects at sterility**
184 To investigate the cellular cause of transgenerational sterility in *gsp-2(yp14)* and
185 *lab-1* mutants, we examined germline development in animals that became sterile after
186 multiple generations. We previously reported that sterile *rsd-2* and *rsd-6* animals display
187 a wide range of germline sizes, including many with few or no germ cells [12].
188 Interestingly, at the L4 larval stage, we found no significant difference between the
189 germline profiles of *rsd-6* mutants at the generation of sterility and wild-type controls
190 (Fig. 2H, Table S3). Most sterile generation L4 *gsp-2(yp14)* and *lab-1* mutant germlines
191 were normal in size, though a small minority had a reduction in total germline length,
192 resulting in a weak but significant difference in germline profile compared to wild-type
193 (Fig. 2H, Table S3). Differentiating germ cell nuclei in spermatogenesis were observed
194 for sterile generation L4 larvae for all strains (Fig. 2A,H). However, the germlines of two-
195 day-old sterile *gsp-2*, *lab-1* and *rsd-6* mutant adults ranged in size from normal to a
196 complete loss of germ cells (Fig. 2B-E,H), resulting in a strong significant difference
197 when compared to wild-type controls (Table S3 p<1E-80). Given the similarities
198 between the RNAi defective mutant *rsd-6* and *gsp-2*, we studied two additional small
199 RNA silencing mutants. The germline profiles of adult sterile-generation *hrde-1* and

nrde-2 were similar to sterile *gsp-2(yp14)* animals (Fig. 2H, Table S2). Similar to *gsp-2* and *lab-1* mutants, *hrde-1* or *nrde-2* mutant L4 larvae that were poised to become sterile displayed predominantly normal-sized germlines (Fig. 2H). We previously showed that mutations in the cell death genes *ced-3* and *ced-4* partially rescued the empty and atrophy phenotypes observed for germlines of *rsd-2* and *rsd-6* small RNA silencing mutant adults [12], suggesting that apoptosis promotes germ cell atrophy as these animals develop from L4 larvae into adults.

Acute loss of GSP-2 does not cause small RNA mutant germline phenotypes

Previous work on GSP-2 in *C. elegans* reported that offspring of *gsp-2(tm301)* F2 homozygotes exhibited 98% embryonic lethality and that sterility occurred for F3 escapers [28,30]. To determine if acute loss of GSP-2 causes germline atrophy, we examined *gsp-2(tm301)* null mutants grown at 20°C and 25°C. We observed high levels of embryonic lethality for F3 embryos (97%), with a few escapers surviving to become uniformly sterile F3 adults that produced no F4 progeny [28] (Fig. 1B). These very high levels of embryonic lethality contrast with 41.6% embryonic lethality seen in *gsp2(yp14)* F8 animals grown at 25°C (Fig. 1B). *gsp2(tm301)* homozygous F2 animals and their few surviving F3 progeny showed normal germlines, with no morphological defects in germline size or development for either L4 larvae or young adults, which significantly differed from the germline profiles of *gsp-2(yp-14)* animals (Table S2, S3). Therefore, the late-generation sterility phenotype of *yp14* mutants is distinct from the fertility defects that occur in response to acute loss of GSP-2 in maternally depleted F3 deletion homozygotes.

A meiotic recombination defect occurs at the generation of sterility

Mature *C. elegans* oocytes typically contain 6 bivalents (pairs of homologous chromosomes held together by crossovers), which can be scored as DAPI-stained bodies. Defects in meiosis can lead to the presence of univalents, which are observed as greater than 6 DAPI bodies per oocyte. We previously observed that small RNA nuclear silencing *mrt* mutants *rsd-2* and *rsd-6* displayed increased levels of univalents at sterility, which were not observed in either wildtype or in fertile *rsd-2* or *rsd-6* mutant late-generation animals grown at 25°C [12]. We measured the presence of univalents in *gsp-2(yp14)* and RNAi mutant strains and found that oocytes of control N2 wildtype or fertile *gsp-2(yp14)* worms grown at 20°C and 25°C almost always contained 6 DAPI bodies representing the 6 paired chromosomes (5 bodies are occasionally scored when bivalents that overlap spatially cannot be distinguished). However, when *gsp-2(yp14)* worms were passaged at 25°C until sterility, only 60% of oocytes containing 6 paired chromosomes with the other 40% containing 7 to 12 DAPI bodies (Fig. 2I). This increase in oocyte univalents was not present in fertile *gsp-2(yp14)* worms, even for late-generation 25°C strains close to sterility (Fig. 2I). We found no univalents in the null *gsp-2* allele *tm301*, either for F2 animals or for rare F3 escapers, consistent with previous observations [28,30]. Together these results emphasize that the germline phenotypes of sterile late-generation *gsp-2(yp14)* animals are distinct from those caused by acute zygotic or maternal loss of GSP-2 [25,26].

Given that LAB-1 and GSP-2 promote meiotic chromosome cohesion, we tested the hypothesis that dysfunction of other factors that promote meiotic chromosome

246 cohesion might be sufficient to elicit germline atrophy. Sterile adults of mutant strains
247 with defects in cohesion, *smc-3(t2553)* and in *coh-3(gk112); coh-4(tm1857)* double
248 mutants [33–35] did not exhibit germline atrophy phenotypes observed in *gsp-2(yp14)*
249 (Fig. S2, Table S2). Therefore, the late-generation sterility phenotypes of *gsp-2(yp14)*
250 and small RNA mutants are not due to acute loss of meiotic chromosome cohesion.
251
252 **Increased expression of repetitive DNA in sterile *gsp-2(yp14)* and *rsd-6* mutants**
253 One of the main functions of small RNA-mediated genomic silencing is to
254 maintain silencing of repetitive elements and transposons in the germline, thereby
255 protecting genomic integrity [15,19,36]. Previously, we reported that RNA expression of
256 tandem repeat loci was upregulated in late-generation *rsd-2* and *rsd-6* mutants grown at
257 25°C [12]. Because similar levels of germline atrophy and univalents were observed in
258 multiple small RNA pathway mutants and in *gsp-2(yp14)* at sterility, we asked if
259 desilencing of tandem repeats occurred in *gsp-2(yp14)* mutants. We used RNA
260 fluorescence *in situ* hybridization (FISH) to examine the expression of multiple repetitive
261 elements. In wild-type controls grown at 25°C, we detected RNA from tandem repeat
262 sequences using *CeRep59* sense and anti-sense probes in embryos but not in the adult
263 germline or somatic cells, consistent with previous observations (Fig. 3A,B) [12].
264 However, in late-generation *gsp-2(yp14)* and *rsd-6*, robust expression of tandem
265 repeats was observed throughout the soma and germline of adult animals, indicating
266 that tandem repeats become desilenced in these strains (Fig. 3C-F).
267
268 **Small RNA silencing components and *gsp-2* promote germ cell immortality**

To study the relationship between *gsp-2(yp14)* and the small RNA nuclear silencing pathway, we created double mutants between *gsp-2(yp14)* and small RNA silencing mutants that display temperature-sensitive defects in germ cell immortality, *hrde-1, nrde-2* and *rsd-6.* Because *gsp-2(yp14)* is a hypomorphic allele, we predicted there would be a similar number of generations to sterility if it were functioning in the small RNA silencing pathway. For *gsp-2(yp14); hrde-1* and *rsd-6; gsp-2(yp14)*, we saw a modest decrease in the number of generations to sterility suggesting a slight additive effect (Fig. 4A,C, Log Rank test: p<.0001). In contrast, *nrde-2; gsp-2(yp14)* double mutants did not differ from the single mutants (Fig. 4B, Log Rank test: p=.06). Together, these results indicate that there is a weak additive effect on transgenerational lifespan when *gsp-2* is combined with *hrde-1* or *rsd-6*, but not when it is combined with *nrde-2*, which promotes the accumulation of stalled RNA polymerase II at loci that are targeted by small RNAs. The modest acceleration observed for some small RNA genomic silencing pathway and *gsp-2(yp14)* double mutants may be consistent with a recent report that indicated that epigenetic silencing marks typically overlap imperfectly for epigenomic silencing mutants, such that both shared and unique targets occur [15].

gsp-2(yp14) and _lab-1_ display increased histone H3 phosphorylation

Previously, increased H3S10 phosphorylation was observed when *gsp-2* is deficient [30]. The H3K9me and H3S10p marks can function as a phospho-methyl switch where H3S10 phosphorylation can block some epigenetic regulators, such as HP1, from accessing the adjacent H3K9me mark [37–39]. H3S10 phosphorylation was visible on the condensed chromosomes in the -1 to -3 oocytes in wildtype worms grown

at 20°C and 25°C (Fig. 5A). In both early- and late-generation *gsp-2(yp14)* mutant oocytes, H3S10 phosphorylation increased when compared with wildtype controls, with increased levels on chromosomes (Fig. 5B,M). We observed increased levels of H3S10 phosphorylation in *lab-1* mutants (Fig. 5C,M), consistent with previous results [25]. Increased levels of H3S10p also occurred in *lab-1, rsd-6,* and *hrde-1* but not in *nrde-2* mutants (Fig. 5C-F,M). Late-generation *gsp-2(yp14)* mutant animals grown at 25ºC had a small but significant increase in H3S10 phosphorylation levels compared to *gsp-2(yp14)* mutant controls grown at 20ºC (Fig. 5M).

PP1 has been previously shown to dephosphorylate a number of histone amino acids, including H3T3 [40]. LAB-1 recruits GSP-2/PP1 to dephosphorylate H3T3, which represses the recruitment of Aurora B/AIR-2 to the long arms of *C. elegans* meiotic chromosomes, which separate in Meiosis II, thereby restricting Aurora B-mediated phosphorylation of H3S10 to meiotic short arms, which separate in Meiosis I [25,26,41]. We hypothesized that excess H3T3 phosphorylation could affect the ability of H3K4 demethylases to access H3K4 resulting in a Mrt phenotype similar to *rbr-2* or *spr-5* H3K4 demethylase mutants [42]. When we examined H3T3 phosphorylation in wildtype controls, staining was visible in the -1 to -3 oocytes and was localized to the short arms of meiotic chromosomes, the site of chromosome separation at Meiosis I (Fig. 5G-G'). The long arms, which do not exhibit staining, are analogous to the centromere in mono-centromeric organisms (Fig. 7). However, in *gsp-2(yp14)* mutants, H3T3p staining was expanded to cover the entire chromosome and was significantly brighter when images where taken under the same conditions (Fig. 5H-H'). In contrast to our H3S10p results, *lab-1* and the small RNA mutants *hrde-1, rsd-6* and *nrde-2* all exhibited increased H3T3

315 phosphorylation signal intensity in the -1 to -3 oocytes, although the signal was still
316 localized properly to the short arms of the meiotic chromosomes (Fig. 5I-L,N).
317 Furthermore, there was a significant increase in H3T3 phosphorylation in the sterile
318 generation of *gsp-2(yp14)* mutants compared to the earlier, fertile generation animals
319 suggesting transgenerational accumulation of H3T3 phosphorylation (Fig. 5N).
320 Together, our results suggest that an increase in phosphorylation of H3T3 but not
321 H3S10 consistently occurs in oocytes of *gsp-2* and small RNA silencing mutants. This
322 defect is sensitive to temperature, as observed for the meiotic chromosome segregation
323 and germ cell immortality defects of *gsp-2(yp14)* (Fig. 1E,F).
324
325 **Small RNA-mediated genome silencing is disrupted in *gsp-2(yp14)***
326 Multiple genes that regulate small RNA-mediated epigenomic silencing promote germ
327 cell immortality, including three genes that are required for a form of transcriptional gene
328 silencing termed nuclear RNA interference, *nrde-1*, *nrde-2* and *nrde-4* [10,12,43]. The
329 response to a dsRNA trigger that targets *lin-26* is dependent on nuclear RNA
330 interference [44]. Control wildtype and *gsp-2* mutant animals displayed a completely
331 penetrant Embryonic Lethality phenotype in response to *lin-26* dsRNA, whereas nuclear
332 RNAi defective mutant *nrde-2* and the RNAi defective mutant *rsd-6* did not (Fig. 6A),
333 indicating that nuclear RNAi within a single generation is normal in the *gsp-2* mutant.
334 Small RNAs can trigger RNAi inheritance [10,13], where silencing of a gene in
335 response to siRNAs can be transmitted for multiple generations. Transgenerational
336 RNAi inheritance can occur when endogenous genes are targeted by dsRNA triggers
337 [45], but this can also happen when GFP reporter transgenes are targeted by small

RNAs derived from *GFP*. We tested the transgene *cpIs12* and found that it was silenced in response to GFP siRNAs and that silencing of this transgene was inherited for up to 4 generations after removal from the dsRNA trigger (Fig. 6B). In contrast, GFP expression in *gsp-2(yp14)*; *cpIs12* was initially silenced but silencing was not inherited over multiple generations (Fig. 6B), suggesting that *gsp-2* plays a role in RNAi inheritance.

Propagation of GFP or mCherry transgenes in the heterozygous state for multiple generations can elicit strong transgene silencing [21]. We found that the transgene *cpIs12* was progressively silenced in the population over the course of several generations until fully silenced by generation 5 (Fig. 6C). In contrast, when *cpIs12* was placed in a *gsp-2(yp14)* genetic background and propagated in a heterozygous state, we found that *cpIs12* was initially weakly silenced and that genomic silencing never became fully penetrant (Fig. 6C). Together, the above data indicate that *gsp-2* promotes transgenerational small RNA-induced genome silencing.

Small RNA dysfunction in *gsp-2* mutants

Given that small RNA-mediated genome silencing is dysfunctional in *gsp-2(yp14)* mutants, we asked if small RNA populations were perturbed by preparing RNA from early- and late-generation wildtype, *gsp-2(yp14)*, *rsd-6* and *spr-5* mutants grown at either 20°C or 25°C. *spr-5* encodes an H3K4 demethylase that promotes Germ Cell Immortality at 25°C, similar to *rsd-6* and *gsp-2* mutants [42]. Small RNA libraries were prepared and subjected to high throughput sequencing, and we then examined levels of 22G RNAs that are 22 nucleotides in length beginning with a 5’ guanine, as 22G RNAs are the major effectors of genomic silencing in *C. elegans* [5,46]. Analysis of the small

RNA data revealed that *spr-5* and *rsd-6* share some genes with reduced levels of 22G RNAs with increasing generations, but there are other genes that show dissimilar behavior for each individual mutant. This suggests that *spr-5* may act both in conjunction with *rsd-6* and in a separate pathway to promote germline immortality. In contrast, 22G RNAs from *gsp-2(yp14)* showed strong similarities to those of *spr-5* mutants but showed little similarity to 22G RNA changes observed for *rsd-6* mutants (Fig. 6D and Fig. S3), suggesting that *gsp-2* may act in a separate pathway from *rsd-6*, in agreement with the results from epistasis experiments above. As a control, there is little coherent change in late-generation versus early generation N2 wildtype that overlaps with *gsp-2(yp14)* (Fig. S3). As germ cell immortality is promoted in part by primary siRNAs termed piRNAs that interact with the Piwi Argonaute protein PRG-1 [8], we also examined piRNA populations, which are enriched for 21 nucleotide RNAs that begin with a 5' uracil (21U RNAs) [6,7,9] and found that these were normal (Fig. 6E).

Discussion

We demonstrate for the first time that *gsp-2* and *lab-1* are required for germ cell immortality at 25°C as strains deficient for these proteins can be passaged for a number of generations before becoming sterile (Fig. 1C,D). Although PP1 is a general protein phosphatase with roles in a number of cellular processes including mitosis and meiosis [24], we identified a separation-of-function allele of *gsp-2* that displayed an X chromosome non-disjunction phenotype that was specific for meiosis (Fig. 1B,G). The incidence of both X chromosome loss and inviable embryos, which are likely aneuploid for autosomes, was exacerbated at high temperature (Fig. 1A,B), suggesting that this

meiotic chromosome segregation defect could contribute to the temperature-sensitive nature of the Mrt phenotype of *gsp-2(yp14)*. Consistently, PP1/GSP-2 is recruited to meiotic chromosomes by the *C. elegans*-specific protein LAB-1, and we found that deficiency for *lab-1* elicited transgenerational sterility accompanied by adult germ cell degeneration phenotypes that were observed in sterile small RNA silencing mutants (Fig. 1F and Fig 2). Together, these results indicate that LAB-1 and GSP-2/PP1 define a step during meiosis that is critical for potentiating transgenerational small RNA-mediated genome silencing and germ cell immortality (Fig. 7A).

LAB-1 localizes to the interface between homologous chromosomes during pachytene, and LAB-1 recruits GSP-2 to nuclei during early stages of meiosis (Fig. 7A) (de Carvalho et al., 2008; Tzur et al., 2012). Moreover, deficiency for LAB-1 perturbs the pairing of homologous chromosomes during meiosis, which has been attributed to a defect in the cohesion of sister chromatids (Tzur et al., 2012). We suggest that a previously undescribed function of LAB-1/GSP-2, potentially related to the pairing of homologous chromosomes, may act at the interface between homologs to promote small RNA-mediated epigenomic silencing (Fig. 7A). We found that persistent transgenerational discontinuities in the pairing of homologous chromosomes during meiosis, caused by hemizygous transgenes, can promote transgene silencing in a manner that depends on GSP-2 (Fig. 6C, Fig. 7C). This hemizygous transgene silencing process occurs in a manner that depends *prg-1*/piRNAs as well as downstream factors that promote second siRNA biogenesis [21]. However, we found that piRNA levels were normal in *gsp-2(yp14)* mutants, and also that late-generation *gsp-2(yp14)* strains displayed changes in 22G RNA levels that were similar to those of

407 *spr-5* histone H3K4 demethylase mutants but not to those of *rsd-6* small RNA
408 biogenesis mutants (Fig. 6D and Fig. S3). Moreover, epistasis analysis indicated that
409 there is a weak additive effect when *gsp-2* is combined with the nuclear Argonaute
410 *hrde-1* or the small RNA biogenesis factor *rsd-6,* but no additive effect when *gsp-2* is
411 combined with *nrde-2* (Fig. 4), which like *spr-5* functions downstream of siRNAs to
412 promote transcriptional silencing [47]. The parallel with *spr-5* mutant small RNA levels
413 suggests that GSP-2 help to integrate histone silencing modifications with the response
414 to small RNAs (Fig. 7B). An intriguing possibility is that hemizygous transgenes could
415 create a structural discontinuity between homologous chromosomes that alter the
416 normal meiotic function of LAB-1/GSP-2, creating an environment where the
417 chromosome silencing machinery can respond to small RNAs (Fig. 7C). Alternatively,
418 the presence of a homologous allele could provide protection from silencing [48–50].
419 These possibilities are consistent with a role for small RNA-mediated genome silencing
420 in responding to structures of *de novo* transposon insertions that present a threat to
421 genomic integrity and that might create small hemizygous chromosome pairing
422 aberrations during meiosis, which would be structurally analogous to hemizygous
423 transgenes (Fig. 7C).

424 Consistent with our results, an allele of the *Drosophila* Protein Phosphatase 1
425 gene, *Su var (3) 6*, was identified as a suppressor of position-effect variegation, which
426 relieves epigenetic silencing of a transcriptionally active gene that is placed adjacent to
427 a segment of heterochromatin [29]. As position-effect variegation is promoted by small
428 RNA-mediated genome silencing in plants and animals [51,52], we conclude that PP1 is
429 likely to play a conserved role in this epigenomic silencing process. It has been

suggested that the heterochromatin defect of *Su var (3) 6* mutants could reflect a direct role of PP1 in dephosphorylation of H3S10p, a mark that results in dissociation of Heterochromatin Protein 1 from heterochromatin [40,41]. Moreover, human PP1 has been shown to dephosphorylate H3T3p, this function is also carried out by *C. elegans* GSP-2 during meiosis [40,41]. One or both of these silencing marks could be relevant to meiotic small RNA-mediated genome silencing. Interestingly, the cohesin complex has been found to be recruited to silent chromatin, but in most cases has not been found to be necessary for genomic silencing [53]. As GSP-2 plays a role in protecting cohesin from being prematurely removed, it is likely localized to silent chromatin where it may play a role in maintaining silencing.

We observed increased H3T3 and H3S10 phosphorylation in mature oocytes of *gsp-2(yp14)* mutants as well as in small RNA genome silencing mutants. While the H3 phosphorylation defects that we observed were mildly sensitive to temperature, *gsp-2(yp14)* displayed more pronounced H3 phosphorylation defects that spread along the length of meiotic chromosomes, whereas small RNA mutants displayed proper H3 phosphorylation localization whose intensity was consistently stronger than for wildtype controls for H3T3 but not for H3S10 (Fig. 5). Given that LAB-1/GSP-1 localize to sister chromosomes in mature oocytes that are arrested in Meiosis I, where homologous chromosomes are held together only by crossovers, we propose that the role of LAB-1/GSP-2 in genome silencing may be at earlier stages of meiosis where the homologs are paired in a manner that might be capable of responding to discontinuities between homologs. We suggest that the changes in H3T3 phosphorylation of genome silencing mutants could reflect an indirect effect of dysregulation of heterochromatin, for example

453 a response to altered levels of genome-wide levels of H3K9 methylation could affect the
454 activity of protein that functions in the context of heterochromatin, such as the H3T3
455 kinase Haspin [43]. As H3T3 phosphorylation is constitutively disrupted in maturing
456 oocytes of the genomic silencing mutants we studied, especially in *gsp-2* and *lab-1*
457 mutants, it is also possible that this phosphorylation mark plays a role in genomic
458 silencing itself.

459 While piRNAs and associated small RNA-mediated genome silencing have been
460 well defined as functioning primarily in the germ line, our study suggests a novel
461 connection between a meiotic process where Piwi-associated small RNAs scan
462 homologous chromosomes for relatively small changes to their primary structure and
463 germ cell immortality. This concept is well supported by work in other organisms,
464 particularly in various fungi and *Drosophila*, where it has been shown that regions of
465 heterozygosity are prone to silencing during meiosis in a small RNA dependent manner
466 (reviewed by [20]). It is also possible that the GSP-2 protein phosphatase promotes
467 small RNA-mediated genome silencing by directly modifying histones or a component of
468 the genome silencing machinery that responds to small RNAs. In principle, our study
469 defines a meiotic process that may intimately link transgenerational small RNA-
470 mediated genome silencing with the structure of paired homologous chromosomes
471 during meiosis. Given that endogenous small RNAs promote germ line stem cell
472 maintenance, oogenesis and meiosis itself [54,55], we suggest that small RNA
473 pathways and germ cell development have evolved to become mutually reinforcing
474 processes.
475

Materials and Methods

Strains:

All strains were cultured at 20°C or 25°C on Nematode Growth Medium (NGM) plates seeded with *E. coli* OP50. Strains used include Bristol N2 wild type, *gsp-2(tm301) III, gsp-2(yp14) III, lab-1(tm1791) I, cpIs12[Pmex-5::GFP::tbb-2 3'UTR + unc-119(+)] II, hrde-1(tm1200) III, rsd-6(yp11) I, nrde-2(gg95) II, rbr-2(tm1231) IV, smc-3(t2553) III, coh-4(tm1857) V, coh-3(gk112) V, air-2(or207) I, unc-32(e189) III, unc-13(e450) I, unc-24(e1172) IV.*

Germline Mortality Assay:

Worms were assessed for the Mortal Germline phenotype using the assay previously described [2]. L1 or L2 larvae were transferred for all assays. After passaging plates that yielded no additional L1 animals were marked as sterile. Log-rank analysis was used to determine differences of transgenerational lifespan between strains.

DAPI staining:

DAPI staining was performed as previously described. L4 larvae were selected from sibling plates and sterile adults were singled as late L4s, observed 24 hours later for confirmed sterility, and then stained 48 hours after collection.

RNA FISH:

DNA oligonucleotide probes coupled with a 5′ Cy5 fluorophore were used to detect repetitive element expression. The four probes used in this study were as follows: tttctgaaggcagtaattct*, CeRep59* on chromosome *I* (located at 4281435–4294595 nt); agaattactgccttcagaaa, antisense *CeRep59* on chromosome *I*; caactgaatccagctcctca, chromosome *V* tandem repeat (located at 8699155–8702766 nt); and gcttaagttcagcgggtaat, 26S rRNA. The strains used for RNA FISH experiments were *rsd-6(yp11)*, *gsp-2(yp14)*, and N2 Bristol wild type. Staining was performed as described by Sakaguchi et al., 2014.

Immunofluorescence:

Adult hermaphrodites raised at 20°C or 25°C were dissected in M9 buffer and flash frozen on dry ice before fixation for 1 min in methanol at -20°C. After washing in PBS supplemented with 0.1% Tween-20 (PBST), primary antibody diluted in in PBST was used to immunostain overnight at 4 °C in a humid chamber. Primaries used were 1:500 pH3S10 (Millipore, 06570), 1:4000 pH3T3 (Cell Signaling, D5G1I, Rabbit) and 1:50 OIC1D4 (Developmental Studies Hybridoma Bank). Secondary antibody staining was performed by using an Cy3 donkey anti-mouse or Cy-5 donkey anti-rabbit overnight at 4°C. All images were obtained using a LSM 710 laser scanning confocal and were taken using same settings as control samples. Images processed using ImageJ. Intensity quantification was done by measuring total fluorescence in individual condensed chromosomes and subtracting the background levels obtained from mitotic nuclei as nucleoplasm levels varied greatly.

RNAi Assays: N2 wildtype, *gsp-2*, *rsd-6* and *nrde-2* animals were grown on *lin-26* RNAi clones and the progeny of 10 worms each were scored for Embryonic Lethality.

Transgene silencing assay: *cpIs12* and *gsp-2; cpIs12* worms were scored for GFP expression on NGM plates and then transferred to RNAi plates targeting GFP. The next generation (that was laid on GFPi plates) were scored for GFP expression and their sisters were removed and transferred back to NGM plates. Worms were propagated for multiple generations on NGM and scored each time for GFP expression. Both GFP reporter *gsp-2* doubles were created by marking with *dpy-17*.

Heterozygous transgene silencing: *cpIs12* was maintained as a heterozygote over *dpy-10 unc-4* while in *gsp-2; cpIs12* doubles, *gsp-2* remained mutant for the entire assay and *cpIs12* was balanced over *dpy-10 unc-4*.

Genome sequence analysis:

Paired sequence reads (2X100 nucleotide long) were mapped to the C. elegans reference genome version WS230 (www.wormbase.org) using the short-read aligner BWA [56]. The resulting alignment files were sorted and indexed with the help of the SAMtools toolbox [57]. The average sequencing depths for the mutant and wild-type N2 strains were 116x and 71x, respectively. Single-nucleotide variants (SNVs) were identified and filtered with SAMtools and annotated with a custom Perl script using gene information downloaded from WormBase WS230. Candidate SNVs in the mutant strain already present in the N2 strain were eliminated from further consideration.

The raw sequence data from this study have been submitted to the NCBI BioProject (http://www.ncbi.nlm.nih.gov/bioproject) under accession number PRJNA395732 and can be accessed from the Sequence Read Archive (SRA; https://www.ncbi.nlm.nih.gov/sra) with accession number SRP113543.

Small RNA Sequence Analysis

5' independent small RNA sequencing was performed as described previously [13], using one repeat for each time-point of N2 WT, *rsd-6* and *spr-5* at 25°C. Custom Perl scripts were used to select different small RNA species from the library. To map small RNA sequences to genes, reads were aligned to the *C. elegans* ce6 genome using Bowtie, Version 0.12.7, requiring perfect matches [58]. Data was normalized to the total number of aligned reads and 1 was added to the number of reads mapping to each gene to avoid division by zero errors. To map 22G sequences to transposons and tandem repeats, direct alignment to the transposon consensus sequences, downloaded from Repbase (Ver 17.05) or repeats obtained from the ce6 genome (WS190) annotations downloaded from UCSC as above, was performed using Bowtie allowing up to two mismatches and reporting only the best match. Uncollapsed fasta files were used for these alignments to compensate for the problem of multiple identical matches. Data was normalized to the total library size and 1 was added to the number of reads mapping to each feature to avoid division by zero errors. In order to analyze data from *rsd-2* mutants grown at 20°C [59], Fasta files were downloaded from the Gene Expression Omnibus and uncollapsed using a custom Perl script before aligning to transposons or tandem repeats as above. Analysis of data was carried out using the R statistical language [60].

Acknowledgements

We thank Jonathan Hodgkin for mapping assistance and members of the S.A. laboratory for critical review of the manuscript. Some strains were provided by the Caenorhabditis Genetics Center, which is funded by National Institutes of Health Office of Research Infrastructure Programs (P40 OD010440). Work in the DM laboratory is funded by the Canadian Institute for Health Research. This work was supported by National Institute of Health grant numbers F32 GM120809 (K.B) and RO1 GM083048 (S.A). SA is a recipient of a Senior Scholar in Aging Award from the Ellison Medical Foundation. Work in PS laboratory is funded by the Medical Research Council. PS holds an Imperial College Research Fellowship.

References

1. Sharpless NE, DePinho RA. How stem cells age and why this makes us grow old. Nat Rev Mol Cell Biol [Internet]. 2007 Sep [cited 2017 Jun 26];8(9):703–13. Available from: http://www.ncbi.nlm.nih.gov/pubmed/17717515
2. Ahmed S, Hodgkin J. MRT-2 checkpoint protein is required for germline immortality and telomere replication in C. elegans. Nature [Internet]. 2000 Jan 13 [cited 2015 Nov 30];403(6766):159–64. Available from: http://www.ncbi.nlm.nih.gov/pubmed/10646593
3. Armanios M, Blackburn EH. The telomere syndromes. Nat Rev Genet [Internet]. 2012 Sep 11 [cited 2017 Jun 26];13(10):693–704. Available from: http://www.ncbi.nlm.nih.gov/pubmed/22965356
4. Meier B, Clejan I, Liu Y, Lowden M, Gartner A, Hodgkin J, et al. trt-1 is the Caenorhabditis elegans catalytic subunit of telomerase. PLoS Genet [Internet]. 2006 Feb 10 [cited 2015 Nov 16];2(2):e18. Available from: http://dx.plos.org/10.1371/journal.pgen.0020018
5. Bagijn MP, Goldstein LD, Sapetschnig A, Weick EM, Bouasker S, Lehrbach NJ, et al. Function, targets, and evolution of Caenorhabditis elegans piRNAs. Science (80-) [Internet]. 2012 Aug 3 [cited 2017 Jun 26];337(6094):574–8. Available from: http://www.ncbi.nlm.nih.gov/pubmed/22700655
6. Batista PJ, Ruby JG, Claycomb JM, Chiang R, Fahlgren N, Kasschau KD, et al. PRG-1 and 21U-RNAs interact to form the piRNA complex required for fertility in C. elegans. Mol Cell [Internet]. 2008 Jul 11 [cited 2017 Jul 5];31(1):67–78. Available from: http://www.ncbi.nlm.nih.gov/pubmed/18571452
7. Das PP, Bagijn MP, Goldstein LD, Woolford JR, Lehrbach NJ, Sapetschnig A, et al. Piwi and piRNAs Act Upstream of an Endogenous siRNA Pathway to Suppress Tc3 Transposon Mobility in the Caenorhabditis elegans Germline. Mol Cell [Internet]. 2008 Jul 11 [cited 2017 Jun 26];31(1):79–90. Available from: http://www.ncbi.nlm.nih.gov/pubmed/18571451
8. Simon M, Sarkies P, Ikegami K, Doebley A-L, Goldstein LD, Mitchell J, et al. Reduced insulin/IGF-1 signaling restores germ cell immortality to Caenorhabditis elegans Piwi mutants. Cell Rep [Internet]. 2014 May 8 [cited 2015 Nov 11];7(3):762–73. Available from: http://www.pubmedcentral.nih.gov/articlerender.fcgi?artid=4049074&tool=pmcentr

ez&rendertype=abstract
9. Wang G, Reinke V. A C. elegans Piwi, PRG-1, Regulates 21U-RNAs during Spermatogenesis. Curr Biol [Internet]. 2008 Jun 24 [cited 2018 Feb 6];18(12):861–7. Available from: http://www.ncbi.nlm.nih.gov/pubmed/18501605
10. Buckley BA, Burkhart KB, Gu SG, Spracklin G, Kershner A, Fritz H, et al. A nuclear Argonaute promotes multigenerational epigenetic inheritance and germline immortality. Nature [Internet]. 2012 Jul 18 [cited 2017 Jun 26];489(7416):447–51. Available from: http://www.nature.com/doifinder/10.1038/nature11352
11. Juliano C, Wang J, Lin H. Uniting Germline and Stem Cells: The Function of Piwi Proteins and the piRNA Pathway in Diverse Organisms. Annu Rev Genet [Internet]. 2011 Dec 15 [cited 2017 Jun 26];45(1):447–69. Available from: http://www.ncbi.nlm.nih.gov/pubmed/21942366
12. Sakaguchi A, Sarkies P, Simon M, Doebley A-L, Goldstein LD, Hedges A, et al. Caenorhabditis elegans RSD-2 and RSD-6 promote germ cell immortality by maintaining small interfering RNA populations. Proc Natl Acad Sci U S A [Internet]. 2014 Oct 14 [cited 2017 Jun 26];111(41):E4323-31. Available from: http://www.ncbi.nlm.nih.gov/pubmed/25258416
13. Ashe A, Sapetschnig A, Weick E-M, Mitchell J, Bagijn MP, Cording AC, et al. piRNAs can trigger a multigenerational epigenetic memory in the germline of C. elegans. Cell [Internet]. 2012 Jul 6 [cited 2017 Jun 26];150(1):88–99. Available from: http://www.ncbi.nlm.nih.gov/pubmed/22738725
14. Burkhart KB, Guang S, Buckley BA, Wong L, Bochner AF, Kennedy S. A pre-mRNA-associating factor links endogenous siRNAs to chromatin regulation. PLoS Genet [Internet]. 2011 Aug [cited 2017 Jun 26];7(8):e1002249. Available from: http://www.ncbi.nlm.nih.gov/pubmed/21901112
15. McMurchy AN, Stempor P, Gaarenstroom T, Wysolmerski B, Dong Y, Aussianikava D, et al. A team of heterochromatin factors collaborates with small RNA pathways to combat repetitive elements and germline stress. Elife [Internet]. 2017 Mar 15 [cited 2017 Jun 26];6. Available from: http://elifesciences.org/lookup/doi/10.7554/eLife.21666
16. Spracklin G, Fields B, Wan G, Vijayendran D, Wallig A, Shukla A, et al. Identification and Characterization of Caenorhabditis elegans RNAi Inheritance Machinery. Genetics [Internet]. 2017 [cited 2017 Jun 29]; Available from: http://www.genetics.org/content/early/2017/05/22/genetics.116.198812
17. Luteijn MJ, van Bergeijk P, Kaaij LJT, Almeida MV, Roovers EF, Berezikov E, et al. Extremely stable Piwi-induced gene silencing in *Caenorhabditis elegans*. EMBO J [Internet]. 2012 Aug 15 [cited 2017 Jun 26];31(16):3422–30. Available from: http://emboj.embopress.org/cgi/doi/10.1038/emboj.2012.213
18. Shirayama M, Seth M, Lee H-C, Gu W, Ishidate T, Conte D, et al. piRNAs Initiate an Epigenetic Memory of Nonself RNA in the C. elegans Germline. Cell [Internet]. 2012 Jul 6 [cited 2017 Jun 26];150(1):65–77. Available from: http://www.ncbi.nlm.nih.gov/pubmed/22738726
19. Zeller P, Padeken J, van Schendel R, Kalck V, Tijsterman M, Gasser SM. Histone H3K9 methylation is dispensable for Caenorhabditis elegans development but suppresses RNA:DNA hybrid-associated repeat instability. Nat Genet [Internet].

2016 Sep 26 [cited 2017 Jun 29];48(11):1385–95. Available from: http://www.ncbi.nlm.nih.gov/pubmed/27668659

20. Kelly WG, Aramayo R. Meiotic silencing and the epigenetics of sex. Chromosom Res [Internet]. 2007 [cited 2018 Jan 29];(15):633–651. Available from: https://link.springer.com/content/pdf/10.1007/s10577-007-1143-0.pdf
21. Leopold LE, Heestand BN, Seong S, Shtessel L, Ahmed S. Lack of pairing during meiosis triggers multigenerational transgene silencing in Caenorhabditis elegans. Proc Natl Acad Sci U S A [Internet]. 2015 May 19 [cited 2015 Nov 16];112(20):E2667-76. Available from: http://www.ncbi.nlm.nih.gov/pubmed/25941370
22. Chu DS, Liu H, Nix P, Wu TF, Ralston EJ, Yates III JR, et al. Sperm chromatin proteomics identifies evolutionarily conserved fertility factors. Nature [Internet]. 2006 Sep 7 [cited 2017 Jun 26];443(7107):101–5. Available from: http://www.ncbi.nlm.nih.gov/pubmed/16943775
23. Wu J -c., Go AC, Samson M, Cintra T, Mirsoian S, Wu TF, et al. Sperm Development and Motility are Regulated by PP1 Phosphatases in Caenorhabditis elegans. Genetics [Internet]. 2012 Jan 1 [cited 2017 Jun 26];190(1):143–57. Available from: http://www.ncbi.nlm.nih.gov/pubmed/22042574
24. Ceulemans H, Bollen M. Functional Diversity of Protein Phosphatase-1, a Cellular Economizer and Reset Button. Physiol Rev [Internet]. 2004 [cited 2017 Jun 26];84(1). Available from: http://physrev.physiology.org/content/84/1/1
25. de Carvalho CE, Zaaijer S, Smolikov S, Gu Y, Schumacher JM, Colaiacovo MP. LAB-1 antagonizes the Aurora B kinase in C. elegans. Genes Dev [Internet]. 2008 Oct 15 [cited 2017 Jun 12];22(20):2869–85. Available from: http://www.ncbi.nlm.nih.gov/pubmed/18923084
26. Tzur YB, Egydio de Carvalho C, Nadarajan S, Van Bostelen I, Gu Y, Chu DS, et al. LAB-1 Targets PP1 and Restricts Aurora B Kinase upon Entrance into Meiosis to Promote Sister Chromatid Cohesion. Hawley RS, editor. PLoS Biol [Internet]. 2012 Aug 21 [cited 2017 Jun 26];10(8):e1001378. Available from: http://dx.plos.org/10.1371/journal.pbio.1001378
27. Hodgkin J, Horvitz HR, Brenner S. Nondisjunction Mutants of the Nematode CAENORHABDITIS ELEGANS. Genetics [Internet]. 1979 Jan [cited 2017 Jun 28];91(1):67–94. Available from: http://www.ncbi.nlm.nih.gov/pubmed/17248881
28. Sassa T, Ueda-Ohba H, Kitamura K, Harada S, Hosono R. Role of Caenorhabditis elegans protein phosphatase type 1, CeGLC-7B,in metaphase to anaphase transition during embryonic development. Exp Cell Res [Internet]. 2003 Jul 15 [cited 2017 Jun 28];287(2):350–60. Available from: http://linkinghub.elsevier.com/retrieve/pii/S0014482703001575
29. Dombradi V, Axton JM, Barker HM, Cohen PTW. Protein phosphatase 1 activity in Drosophila mutants with abnormalities in mitosis and chromosome condensation. FEBS Lett [Internet]. 1990 Nov 26 [cited 2017 Jun 26];275(1–2):39–43. Available from: http://doi.wiley.com/10.1016/0014-5793%2890%2981434-P
30. Hsu J-Y, Sun Z-W, Li X, Reuben M, Tatchell K, Bishop DK, et al. Mitotic Phosphorylation of Histone H3 Is Governed by Ipl1/aurora Kinase and Glc7/PP1 Phosphatase in Budding Yeast and Nematodes logical changes on the DNA template in an energy. Cell [Internet]. 2000 [cited 2017 Jun 12];102:279–91.

Available from: https://pdfs.semanticscholar.org/ddf3/60514ab900f10f1815057170a4428fea0279.pdf

31. Watanabe Y. Shugoshin: guardian spirit at the centromere. Curr Opin Cell Biol [Internet]. 2005 Dec [cited 2017 Jul 5];17(6):590–5. Available from: http://www.ncbi.nlm.nih.gov/pubmed/16229998
32. Hamant O, Golubovskaya I, Meeley R, Fiume E, Timofejeva L, Schleiffer A, et al. A REC8-Dependent Plant Shugoshin Is Required for Maintenance of Centromeric Cohesion during Meiosis and Has No Mitotic Functions. Curr Biol [Internet]. 2005 May 24 [cited 2017 Jul 5];15(10):948–54. Available from: http://www.ncbi.nlm.nih.gov/pubmed/15916952
33. Severson AF, Ling L, van Zuylen V, Meyer BJ. The axial element protein HTP-3 promotes cohesin loading and meiotic axis assembly in C. elegans to implement the meiotic program of chromosome segregation. Genes Dev [Internet]. 2009 Aug 1 [cited 2017 Jun 26];23(15):1763–78. Available from: http://genesdev.cshlp.org/cgi/doi/10.1101/gad.1808809
34. Hagstrom KA, Holmes VF, Cozzarelli NR, Meyer BJ. C. elegans condensin promotes mitotic chromosome architecture, centromere organization, and sister chromatid segregation during mitosis and meiosis. Genes Dev [Internet]. 2002 Mar 15 [cited 2017 Jun 26];16(6):729–42. Available from: http://www.ncbi.nlm.nih.gov/pubmed/11914278
35. Baudrimont A, Penkner A, Woglar A, Mamnun YM, Hulek M, Struck C, et al. A New Thermosensitive smc-3 Allele Reveals Involvement of Cohesin in Homologous Recombination in C. elegans. Polymenis M, editor. PLoS One [Internet]. 2011 Sep 21 [cited 2017 Jun 26];6(9):e24799. Available from: http://dx.plos.org/10.1371/journal.pone.0024799
36. Holoch D, Moazed D. RNA-mediated epigenetic regulation of gene expression. Nat Rev Genet [Internet]. 2015 Jan 2 [cited 2017 Jun 26];16(2):71–84. Available from: http://www.nature.com/doifinder/10.1038/nrg3863
37. Sabbattini P, Canzonetta C, Sjoberg M, Nikic S, Georgiou A, Kemball-Cook G, et al. A novel role for the Aurora B kinase in epigenetic marking of silent chromatin in differentiated postmitotic cells. EMBO J [Internet]. 2007 Nov 14 [cited 2017 Jun 26];26(22):4657–69. Available from: http://www.ncbi.nlm.nih.gov/pubmed/17948062
38. Sabbattini P, Sjoberg M, Nikic S, Frangini A, Holmqvist P-H, Kunowska N, et al. An H3K9/S10 methyl-phospho switch modulates Polycomb and Pol II binding at repressed genes during differentiation. Mol Biol Cell [Internet]. 2014 Mar [cited 2017 Jun 26];25(6):904–15. Available from: http://www.ncbi.nlm.nih.gov/pubmed/24430871
39. Jeong YS, Cho S, Park JS, Ko Y, Kang Y-K. Phosphorylation of serine-10 of histone H3 shields modified lysine-9 selectively during mitosis. Genes to Cells [Internet]. 2010 Mar [cited 2017 Jun 26];15(3):181–92. Available from: http://www.ncbi.nlm.nih.gov/pubmed/20070858
40. Qian J, Lesage B, Beullens M, Van Eynde A, Bollen M. PP1/Repo-Man Dephosphorylates Mitotic Histone H3 at T3 and Regulates Chromosomal Aurora B Targeting. Curr Biol [Internet]. 2011 May 10 [cited 2018 Jan 28];21(9):766–73.

Available from: http://www.ncbi.nlm.nih.gov/pubmed/21514157
41. Sato-Carlton A, Nakamura-Tabuchi C, Chartrand SK, Uchino T, Carlton PM. Phosphorylation of the synaptonemal complex protein SYP-1 promotes meiotic chromosome segregation. J Cell Biol [Internet]. 2017 Dec 8 [cited 2018 Jan 28];jcb.201707161. Available from: http://www.ncbi.nlm.nih.gov/pubmed/29222184
42. Alvares SM, Mayberry GA, Joyner EY, Lakowski B, Ahmed S. H3K4 demethylase activities repress proliferative and postmitotic aging. Aging Cell [Internet]. 2014 Apr [cited 2017 Jun 26];13(2):245–53. Available from: http://www.ncbi.nlm.nih.gov/pubmed/24134677
43. Burton NO, Burkhart KB, Kennedy S. Nuclear RNAi maintains heritable gene silencing in Caenorhabditis elegans. Proc Natl Acad Sci U S A [Internet]. 2011 Dec 6 [cited 2017 Jun 26];108(49):19683–8. Available from: http://www.ncbi.nlm.nih.gov/pubmed/22106253
44. Guang S, Bochner AF, Pavelec DM, Burkhart KB, Harding S, Lachowiec J, et al. An Argonaute Transports siRNAs from the Cytoplasm to the Nucleus. Science (80-) [Internet]. 2008 Jul 25 [cited 2018 Feb 21];321(5888):537–41. Available from: http://www.ncbi.nlm.nih.gov/pubmed/18653886
45. Vastenhouw NL, Brunschwig K, Okihara KL, Müller F, Tijsterman M, Plasterk RHA. Gene expression: long-term gene silencing by RNAi. Nature [Internet]. 2006 Aug 24 [cited 2017 Jun 26];442(7105):882. Available from: http://www.ncbi.nlm.nih.gov/pubmed/16929289
46. Pak J, Fire A. Distinct populations of primary and secondary effectors during RNAi in C. elegans. Science [Internet]. 2007 Jan 12 [cited 2017 Jun 26];315(5809):241–4. Available from: http://www.ncbi.nlm.nih.gov/pubmed/17124291
47. Guang S, Bochner AF, Burkhart KB, Burton N, Pavelec DM, Kennedy S. Small regulatory RNAs inhibit RNA polymerase II during the elongation phase of transcription. Nature [Internet]. 2010 Jun 13 [cited 2018 Feb 12];465(7301):1097–101. Available from: http://www.ncbi.nlm.nih.gov/pubmed/20543824
48. Wedeles CJ, Wu MZ, Claycomb JM. Protection of germline gene expression by the C. elegans Argonaute CSR-1. Dev Cell [Internet]. 2013 Dec 23 [cited 2017 Jun 29];27(6):664–71. Available from: http://www.ncbi.nlm.nih.gov/pubmed/24360783
49. Conine CC, Moresco JJ, Gu W, Shirayama M, Conte D, Yates JR, et al. Argonautes Promote Male Fertility and Provide a Paternal Memory of Germline Gene Expression in C. elegans. Cell [Internet]. 2013 Dec [cited 2015 Jun 30];155(7):1532–44. Available from: http://www.sciencedirect.com/science/article/pii/S0092867413014839
50. Seth M, Shirayama M, Gu W, Ishidate T, Conte D, Mello CC. The C. elegans CSR-1 argonaute pathway counteracts epigenetic silencing to promote germline gene expression. Dev Cell [Internet]. 2013 Dec 23 [cited 2015 Nov 11];27(6):656–63. Available from: http://www.ncbi.nlm.nih.gov/pubmed/24360782
51. Gandhi SG, Bag I, Sengupta S, Pal-Bhadra M, Bhadra U. Drosophila oncogene Gas41 is an RNA interference modulator that intersects heterochromatin and the small interfering RNA pathway. FEBS J [Internet]. 2015 Jan [cited 2018 Jan 14];282(1):153–73. Available from:

http://www.ncbi.nlm.nih.gov/pubmed/25323651

52. Pal-Bhadra M, Leibovitch BA, Gandhi SG, Chikka MR, Rao M, Bhadra U, et al. Heterochromatic Silencing and HP1 Localization in Drosophila Are Dependent on the RNAi Machinery. Science (80-) [Internet]. 2004 Jan 30 [cited 2018 Jan 14];303(5658):669–72. Available from: http://www.ncbi.nlm.nih.gov/pubmed/14752161

53. Chang C-R, Wu C-S, Hom Y, Gartenberg MR. Targeting of cohesin by transcriptionally silent chromatin. Genes Dev [Internet]. 2005 Dec 15 [cited 2018 Feb 27];19(24):3031–42. Available from: http://www.ncbi.nlm.nih.gov/pubmed/16319193

54. Stein P, Rozhkov N V., Li F, Cárdenas FL, Davydenk O, Vandivier LE, et al. Essential Role for Endogenous siRNAs during Meiosis in Mouse Oocytes. Cohen PE, editor. PLOS Genet [Internet]. 2015 Feb 19 [cited 2018 Feb 4];11(2):e1005013. Available from: http://www.ncbi.nlm.nih.gov/pubmed/25695507

55. Ortogero N, Schuster AS, Oliver DK, Riordan CR, Hong AS, Hennig GW, et al. A Novel Class of Somatic Small RNAs Similar to Germ Cell Pachytene PIWI-interacting Small RNAs. J Biol Chem [Internet]. 2014 Nov 21 [cited 2018 Feb 4];289(47):32824–34. Available from: http://www.ncbi.nlm.nih.gov/pubmed/25320077

56. Li H, Durbin R. Fast and accurate short read alignment with Burrows-Wheeler transform. Bioinformatics [Internet]. 2009 Jul 15 [cited 2018 Feb 11];25(14):1754–60. Available from: http://www.ncbi.nlm.nih.gov/pubmed/19451168

57. Li H, Handsaker B, Wysoker A, Fennell T, Ruan J, Homer N, et al. The Sequence Alignment/Map format and SAMtools. Bioinformatics [Internet]. 2009 Aug 15 [cited 2018 Feb 11];25(16):2078–9. Available from: http://www.ncbi.nlm.nih.gov/pubmed/19505943

58. Langmead B, Trapnell C, Pop M, Salzberg SL. Ultrafast and memory-efficient alignment of short DNA sequences to the human genome. Genome Biol [Internet]. 2009 Mar 4 [cited 2018 Feb 19];10(3):R25. Available from: http://genomebiology.biomedcentral.com/articles/10.1186/gb-2009-10-3-r25

59. Frøkjær-Jensen C, Wayne Davis M, Hopkins CE, Newman BJ, Thummel JM, Olesen S-P, et al. Single-copy insertion of transgenes in Caenorhabditis elegans. Nat Genet [Internet]. 2008 Nov 26 [cited 2018 Feb 11];40(11):1375–83. Available from: http://www.ncbi.nlm.nih.gov/pubmed/18953339

60. R Core Team. R: A language and environment for statistical computing [Internet]. R Foundation for Statistical Computing. Vienna, Austria; 2013. Available from: http://www.r-project.org/

Figure Legends

Figure 1: A hypomorphic mutation in *gsp-2* results in transgenerational sterility phenotype. (A) Incidence of males in *gsp-2(yp14)* was 3.9% at 20°C and increased to 16.8% at 25°C. **(B)** Progeny of *gsp-2(yp14)* animals grown at 20°C 25°C were 6% and 41% Embryonic Lethal, respectively, compared to 97% of *gsp-2(tm301)* progeny (N=20). **(C-D)** *gsp-2(yp14)* was identified to have a G to A mutation in exon 5 by whole genome sequencing. This results in a D to N amino acid substitution in a well conserved region of GSP-2. **(E)** When passaged at 20˚C for many generations N2, *gsp-2(yp14)*, *lab-1* and *lab-1; gsp-2(yp14)* did not exhibit a loss of transgenerational fertility. **(F)** *gsp-2(yp14)* and *lab-1* both exhibited loss of fertility at 25˚C and were completely sterile by generation F17 and F11 respectively. A double mutant of *lab-1;gsp-2* went sterile slightly faster than the individual single mutants and were completely sterile by F10. (N≥40) **(G)** Analysis of incidence of males showed no jackpots of males at in *gsp-2(yp14)* animals. *P<.0001 by T-test.

Figure 2: Germline defects occur in *gsp-2* and temperature-sensitive small RNA mutants at sterility. (A-E) Representative images of DAPI stained germlines passaged at 25°C. Germlines of either L4 (A) or adult control and sterile mutant animals were stained, and the germline size quantified as either normal (B), short (C), atrophied (D) or empty (E). **(H)** Germlines from *gsp-2(yp14)*, *lab-1*, *rsd-6*, *nrde-2* and *hrde-1* mutants were examined and found have mostly normal morphology at the L4 stage but exhibited germline atrophy in adult animals (N≥98). **(F,G,I)** In addition to germline atrophy, *gsp-2(yp14)* animals displayed greater than the wildtype number of 6 DAPI bodies in

oocytes at the generation at sterility in 32% of oocytes (N≥100). **(J)** 100% of adult *gsp-2(tm301)* animals displayed normal germline size by DAPI staining (N=30). P-values present in Table S2 and S3. Scale bar= 10um.

Figure 3: Repetitive regions in the genome are desilenced in *gsp-2(yp14)* animals. **(A-F)** Confocal images of Cy5-labeled RNA FISH probes (green) and DAPI-stained nuclei (blue). **(A,C,E)** RNA FISH probes show expression of Ch V repeats in the germlines of *gsp-2(yp14)* (C) and *rsd-6* (E) animals grown at 25°C and only embryonic expression in wildtype controls (A). **(B,D,F)** Probes against CeRep59 repeats reveal similar germline expression in *gsp-2(yp14)* (D) and *rsd-6* (F) animals and embryo-only expression in wildtype controls (B). All images were taken under the same condition. The germ line is outlined with white line. Scale bar= 30um

Figure 4: Temperature-sensitive small RNAi mutants exhibited similar times to sterility as *gsp-2(yp14)* at 25°C. Germline mortality assays all performed at 25°C **(A)** Both *gsp-2(yp14)* and *hrde-1* animals exhibit similar times to sterility while *gsp-2(yp14);hrde-1* double mutants display a slightly decreased time to sterility. $p < .001$**(B)** *gsp-2(yp14)*, *nrde-2* and *rsd-6;gsp-2(yp14)* animals all go sterile in a similar number of generations. p=.06 **(C)** *gsp-2(yp14)* and *rsd-6* exhibit similar times to sterility while *gsp-2(yp14);rsd-6* double mutants become sterile at a slightly earlier generation. $p <$ .001(N≥40). Significance was tested using a log rank test.

Figure 5: Increased histone phosphorylation is present in *gsp-2(yp14)* oocytes.

880 **(A-F)** Day 2 late stage adults passaged at 25°C stained with an pH3S10 antibody (red)
881 and DAPI marking the DNA (green). All samples were prepared at the same time and
882 imaged using identical settings. **(A)** Wildtype control oocytes show low levels of H3S10p
883 on condensed chromosomes. **(B)** *gsp-2(yp14)* oocytes have increased levels of
884 H3S10p covering the entire chromosomes. **(C, F)** Both *lab-1* and *hrde-1* mutants also
885 display increased levels of H3S10p but *nrde-2* **(D)** and *rsd-6* **(E)** do not. (N≥20**) (G-L)**
886 Day 2 late generation or sterile adults passaged at 25°C stained with an pH3S10
887 antibody (red) and DAPI marking the DNA (green). All samples were prepared at the
888 same time and imaged using identical settings. **(G)** Control oocytes show low levels of
889 localized H3T3p on the short arms of the condensed chromosomes. **(H)** *gsp-2(yp14)*
890 oocytes contain high levels of H3T3p that are expanded to cover the entire condensed
891 chromosome. **(I-L)** *lab-1*, *hrde-1*, *rsd-6* and *nrde-2* all display varying levels of increased
892 H3T3p staining compared to wildtype controls but localization to the short arms is still
893 relatively normal. (N≥20) **(M)** Quantification of fluorescence intensity of H3S10p staining
894 in N2, *gsp-2(yp14)* animals grown at 20°C and 25°C, *rsd-6*, *nrde-2*, *hrde-1*, and *lab-1*
895 shows significant difference in staining intensity between N2 and mutants grown at the
896 same temperature (except for *nrde-2*) and between *gsp-2(yp14)* mutants grown at 20°C
897 and 25°C. (N≥20) **(N)** Quantification of fluorescence intensity of H3T3p staining in N2,
898 *gsp-2(yp14)* animals grown at 20°C and 25°C, *rsd-6*, *nrde-2*, *hrde-1*, and *lab-1* shows
899 significant difference in staining intensity between N2 and mutants grown at the same
900 temperature and between *gsp-2(yp14)* mutants grown at 20°C and 25°C. (N≥20) Scale
901 bar= 10um.
902

Figure 6: GSP-2 promotes multigenerational transgene silencing

(A) *gsp-2(yp14)* mutants do not exhibit single generation RNAi defects while *rsd-6* and *nrde-2* mutants are defective for single generation RNAi. **(B)** *cpIs12* remains undetectable for multiple generations after RNAi treatment. However, in *gsp-2(yp14);cpIs12* animals treated with RNAi cpIs12 only remains undetectable for one generation and by generation 3 exhibit close to wildtype levels of expression. **(C)** When LP138, a GFP transgene, is passaged as a heterozygote for multiple generations it is silenced in the germline. LP138 passaged as a heterozygote in a *gsp-2(yp14)* mutants results in only partial silencing over 5 generations suggesting defective heterozygous transgene silencing. **(D)** Comparison of small RNAs in *rsd-6*, *gsp-2* and *spr-5* mutants showing a great overlap in small RNA identity between *gsp-2* and *spr-5*. **(E)** Graph showing levels of piRNA expression in N2 controls, *rsd-6*, *gsp-2* and *spr-5* mutants at both early (E1) and late (L1) generations grown at 25°C.

Figure 7: A model for the roles of GSP-2 and small RNA-mediated silencing in promoting germline immortality. We propose that both GSP-2 and small RNA-mediated silencing regulation the transgenerational inheritance of the epigenome. When these pathways are disrupted loss of epigenetic regulation can lead to germline atrophy. **A)** GSP-2/LAB-1 promote homolog pairing at the initiation of meiosis between homologous chromosomes during pachytene. **(A')** GSP-2/LAB-1 promote sister chromatid cohesion during prophase. **B)** GSP-2 modulates small RNA silencing machinery promoting small RNA silencing potentially through histone dephosphoryation in a manner that promotes epigenetic silencing, **C)** Previous work has shown that PRG-1 is important for heterozygous transgene silencing (red =active transgene and black

927 =silenced) in a similar manner to GSP-2. GSP-2/LAB-1 could function to silence
928 heterozygous regions of DNA which disrupt meiotic pairing between homologs or
929 cohesion between sister chromatids.
930
931 **Supplemental Figure 1: Mapping and non-complementation test of *gsp-2(yp14)***
932 **(A)** Map of genomic region surrounding *gsp-2* on Chr. *III*. **(B)** Mapping of *gsp-2(yp14)*
933 between *dpy-17* and *unc-32* on Chr. *III* placing *yp14* at -1.08. **(C)** Non-complementation
934 test for Him phenotype between *gsp-2(yp14)* and *gsp-2(tm301)* showed an incidence of
935 males of 5.7% at 20°C.
936
937 **Supplemental Figure 2: Loss of cohesion did not cause germline atrophy**
938 DAPI staining and germline analysis showed no germline atrophy in *smc-3* and *coh-3;*
939 *coh-4* mutants and minor defects in *air-2* animals suggesting loss of chromosome
940 cohesion alone does not cause germline atrophy. (N=30)
941
942 **Supplemental Figure 3: *spr-5* and *gsp-2* show overlap in their small RNA**
943 **populations (A)** Multigenerational inheritance assay using a second transgene *pkIs32*
944 in the background of *hrde-1* and *gsp-2* mutants. **(B-E)** Comparison of small RNAs in
945 *rsd-6*, *gsp-2* and *spr-5* mutants: **(B)** *rsd-6* vs *gsp-2*, **(C)** *spr-5* vs *gsp-2*, **(D)** *rsd-6* vs *spr-*
946 *5* and **(E)** N2 vs *gsp-2*.
947
948
949

	Males	Exp Dead Emb	Exp Live Worms	Obs Dead Emb	Obs Live Worms	p-value
20°C gsp-2(yp14)	164	820	5290	88	1492	<0.0001
25°C gsp-2(yp14)	155	775	964	481	1380	<0.0001

Supplemental Table 1: Expected vs Observed Embryonic Lethality

962

963

	N2	*gsp-2(yp14)*	*lab-1*	*gsp-2(tm301)*	*rsd-6*	*nrde-2*	*hrde-1*	*smc-3*	*coh-3/4*	*air-2*
N2	1	1.008E-85	1.5E-90	1	2E-85	1.3E-67	2E-59	1	1	8.1E-55
gsp-2(yp14)	1E-85	1	5.1E-17	1.646E-45	8E-06	1.4E-06	0.0154	1.2E-40	6.7E-41	5.4E-23
lab-1	2E-90	5.13E-17	1	2.2041E-47	5E-11	1.2E-16	8E-17	7.3E-43	4.4E-43	1.8E-19
gsp-2(tm301)	1	1.646E-45	2.2E-47	1	1E-43	8.2E-32	9E-27	1	1	8.2E-25
rsd-6	2E-85	7.718E-06	4.9E-11	1.3493E-43	1	3.4E-12	9E-11	4E-39	2.5E-39	3.5E-29
nrde-2	1E-67	1.383E-06	1.2E-16	8.175E-32	3E-12	1	0.248	7.5E-28	4.9E-28	8.4E-08
hrde-1	2E-59	0.01536	7.8E-17	9.4732E-27	9E-11	0.248	1	4.1E-23	2.7E-23	7.6E-10
smc-3	1	1.151E-40	7.3E-43	1	4E-39	7.5E-28	4E-23	1	1	1.9E-21
coh-3/4	1	6.658E-41	4.4E-43	1	2E-39	4.9E-28	3E-23	1	1	1.3E-21
air-2	8E-55	5.438E-23	1.8E-19	8.1847E-25	4E-29	8.4E-08	8E-10	1.9E-21	1.3E-21	1

964

965 **Supplemental Table 2: P-values for adult germline defects in *gsp-2* and**

966 **temperature-sensitive small RNA mutants**

967

968

969

	N2	gsp-2(yp14)	lab-1	gsp-2(tm301)	rsd-6	nrde-2	hrde-1
N2	1	2.23E-05	0.036	1	1	0.0031	0.005
gsp-2(yp14)	2.23E-05	1	1	0.00140304	4E-04	1	1
lab-1	0.036421	1	1	0.69600428	0.126	1	1
gsp-2(tm301)	1	0.001403	0.696	1	1	0.0859	0.119
rsd-6	1	0.0003621	0.126	1	1	0.0172	0.024
nrde-2	0.003076	1	1	0.08591014	0.017	1	1
hrde-1	0.00461	1	1	0.11911645	0.024	1	1

970

971 **Supplemental Table 3: P-values for L4 germline defects in *gsp-2* and temperature-**

972 **sensitive small RNA mutants**

973

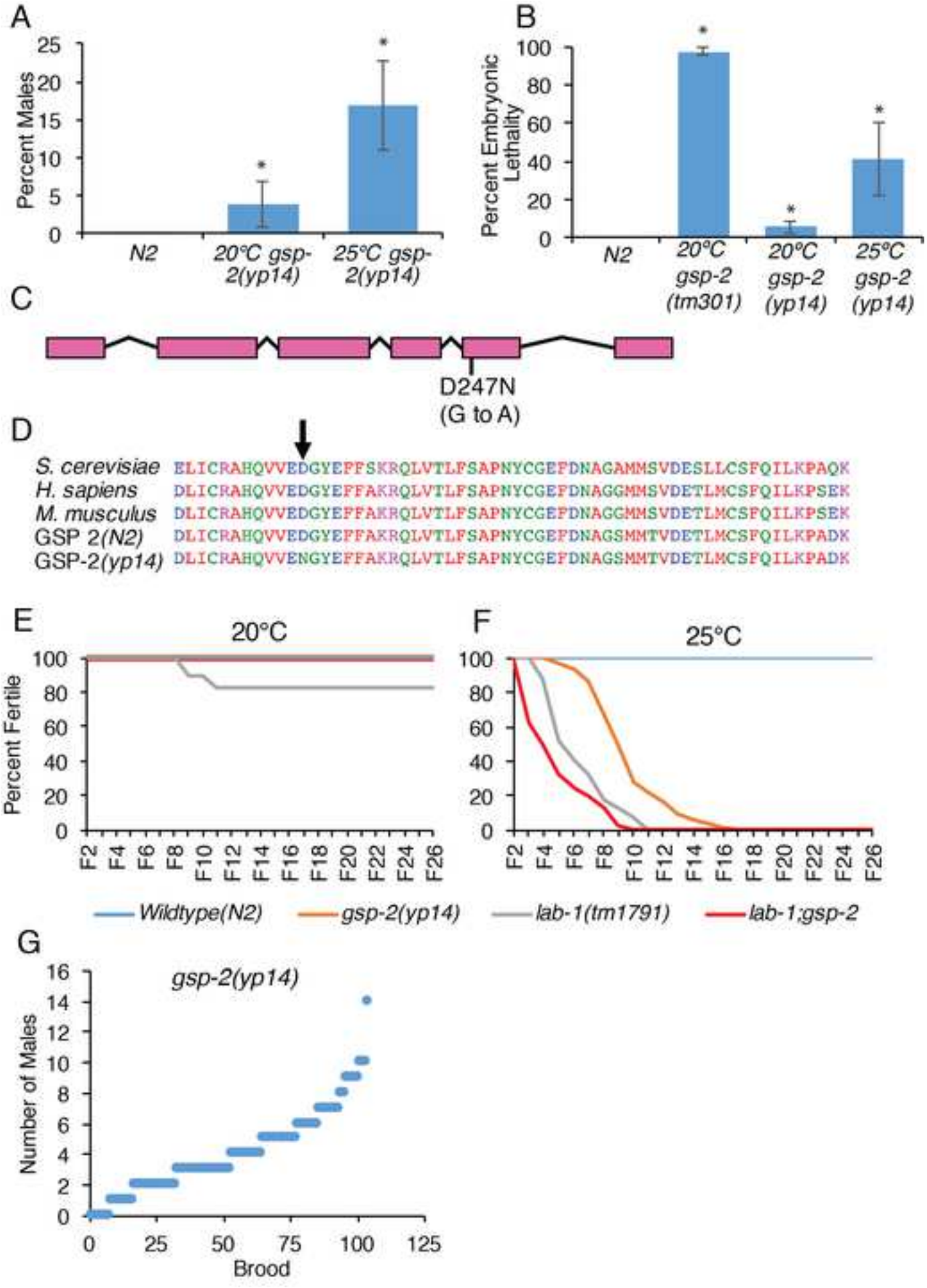

Figure 2

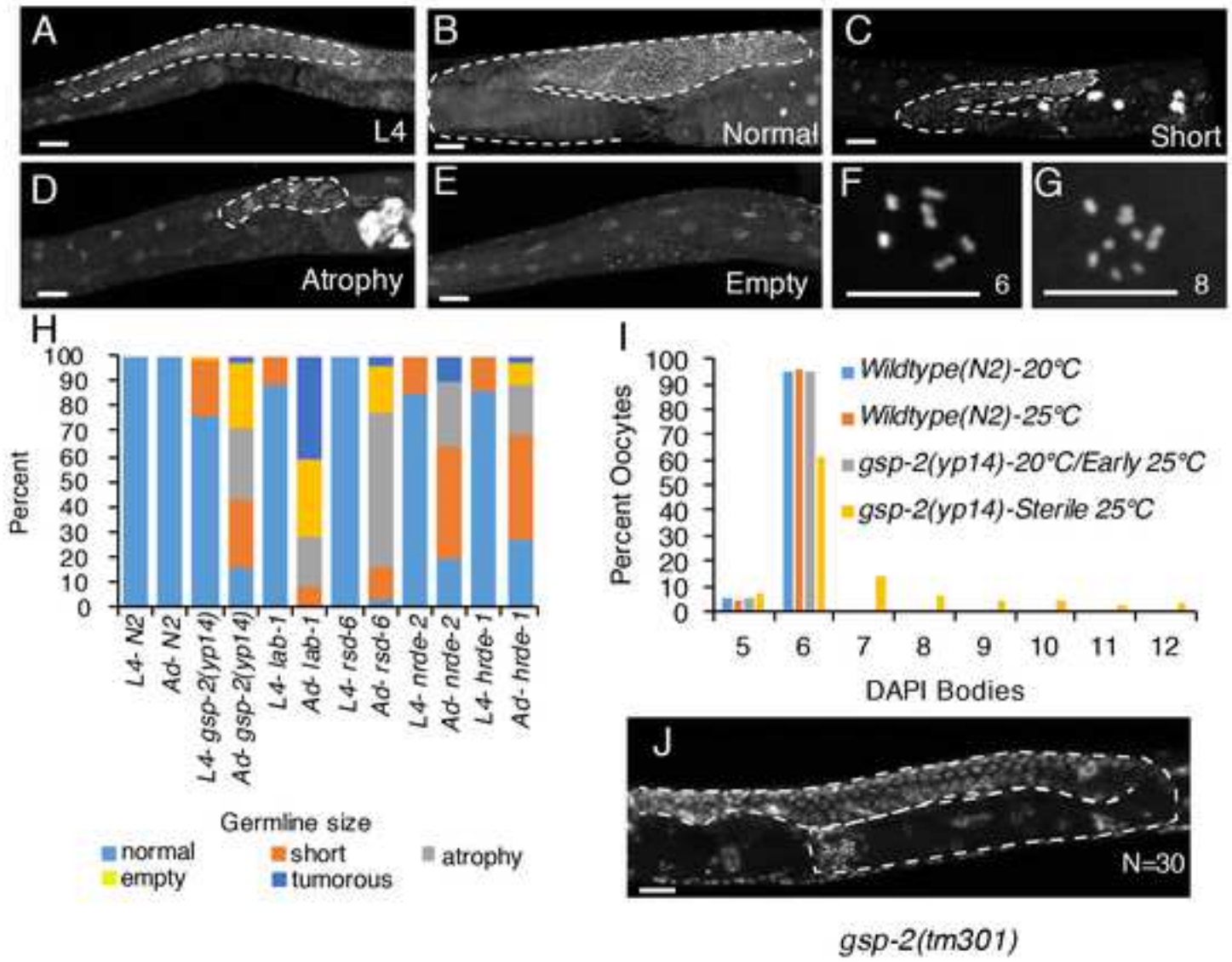

Figure 3

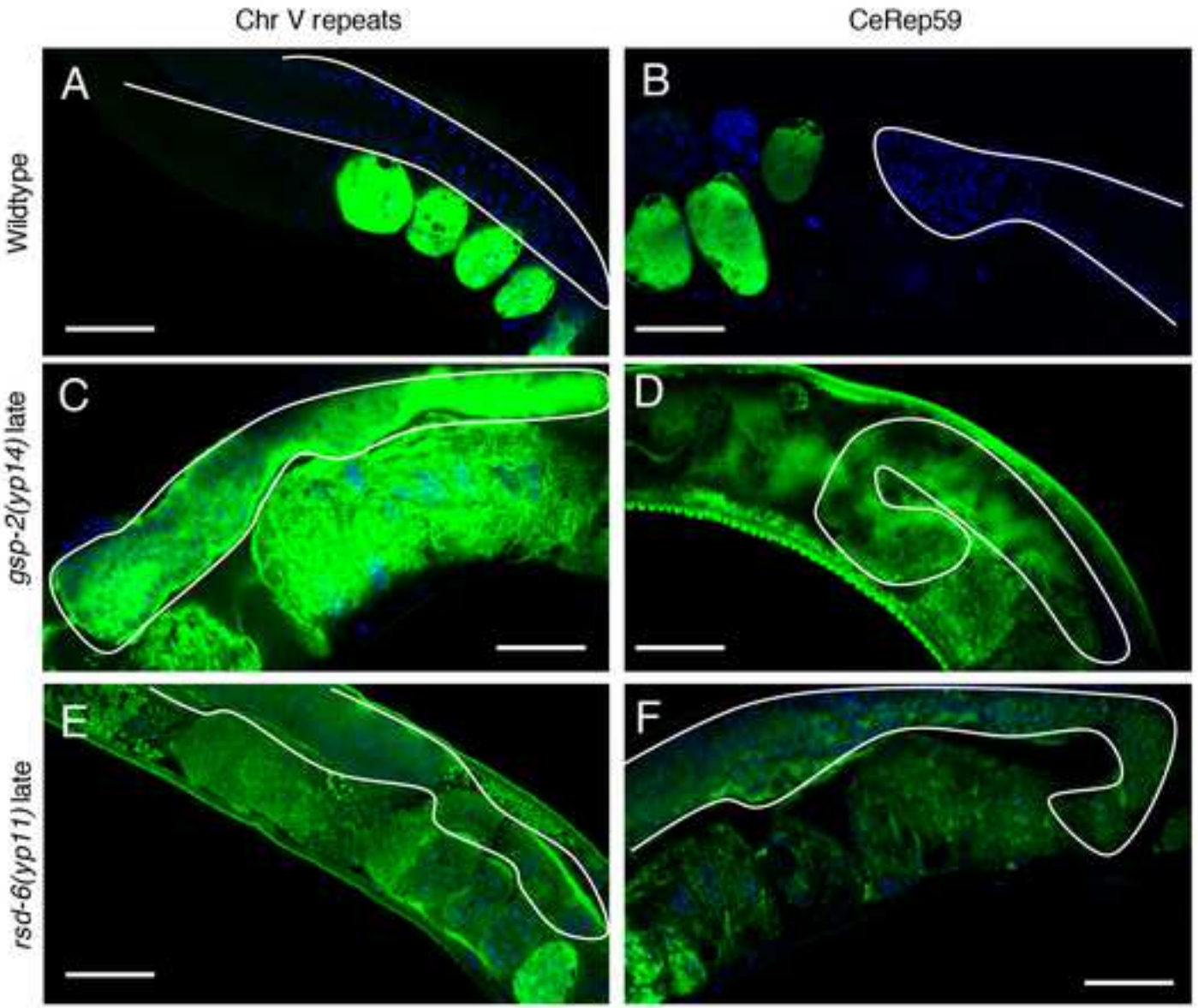

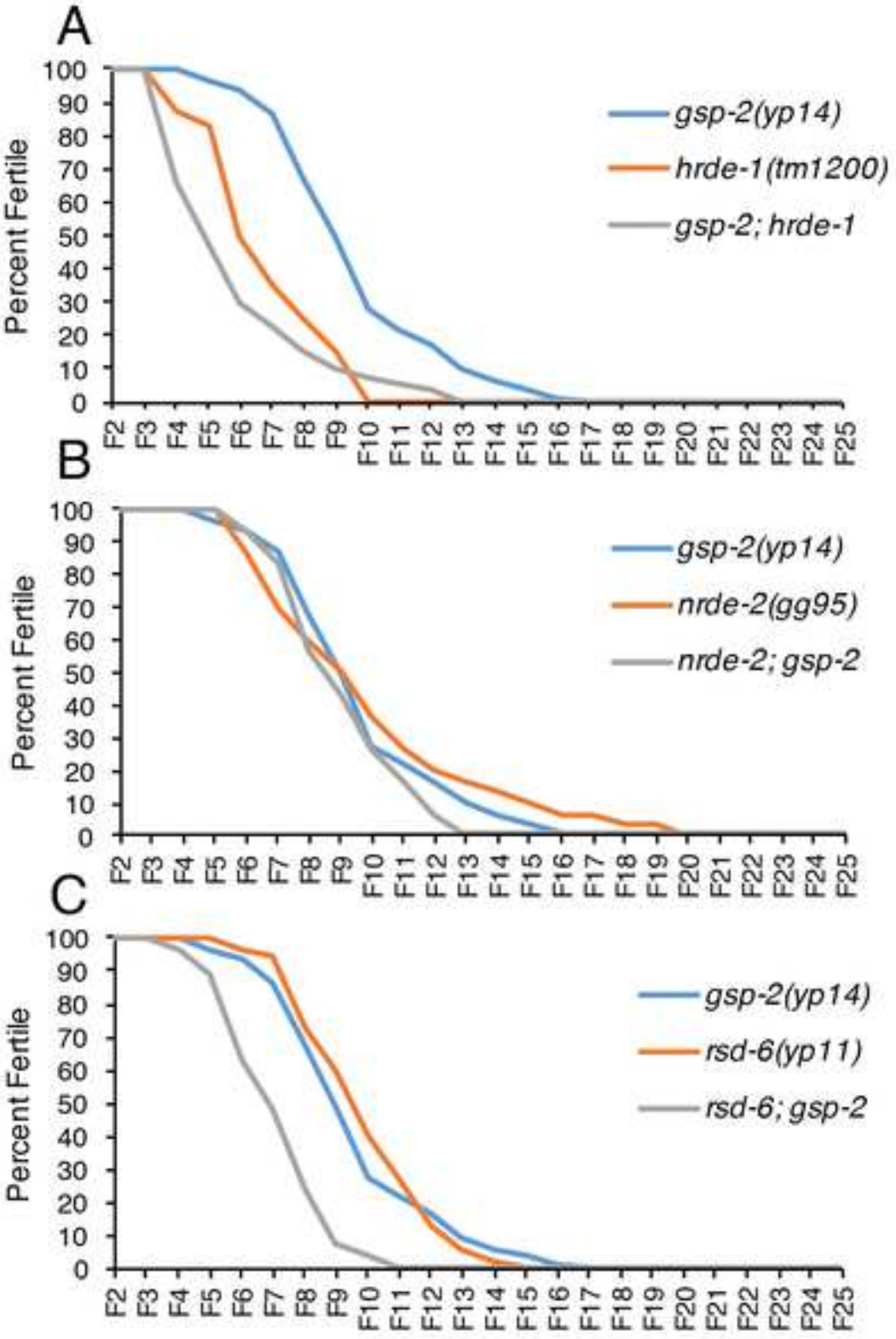

Figure 5

Click here to download Figure fig5.1.tif

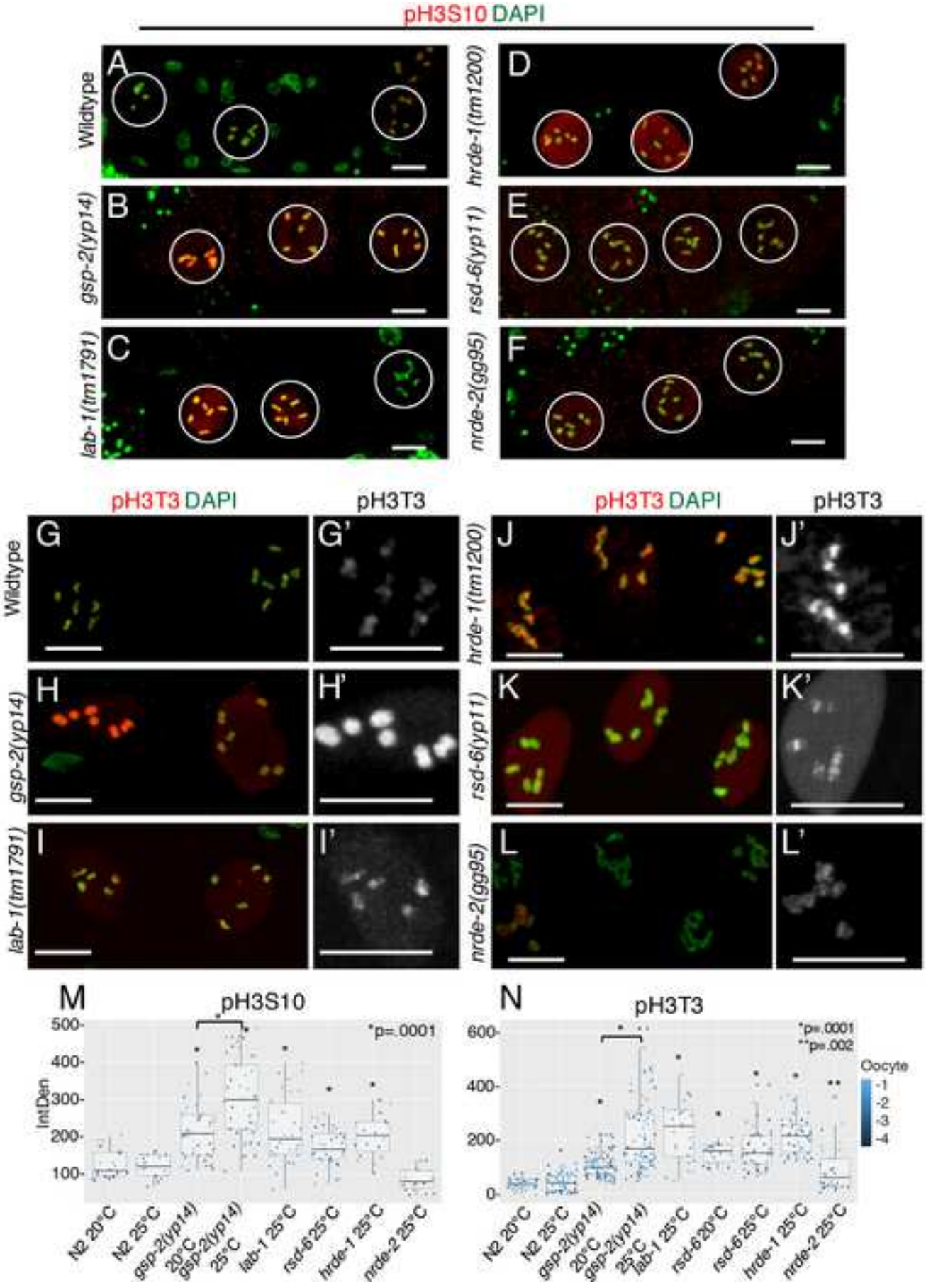

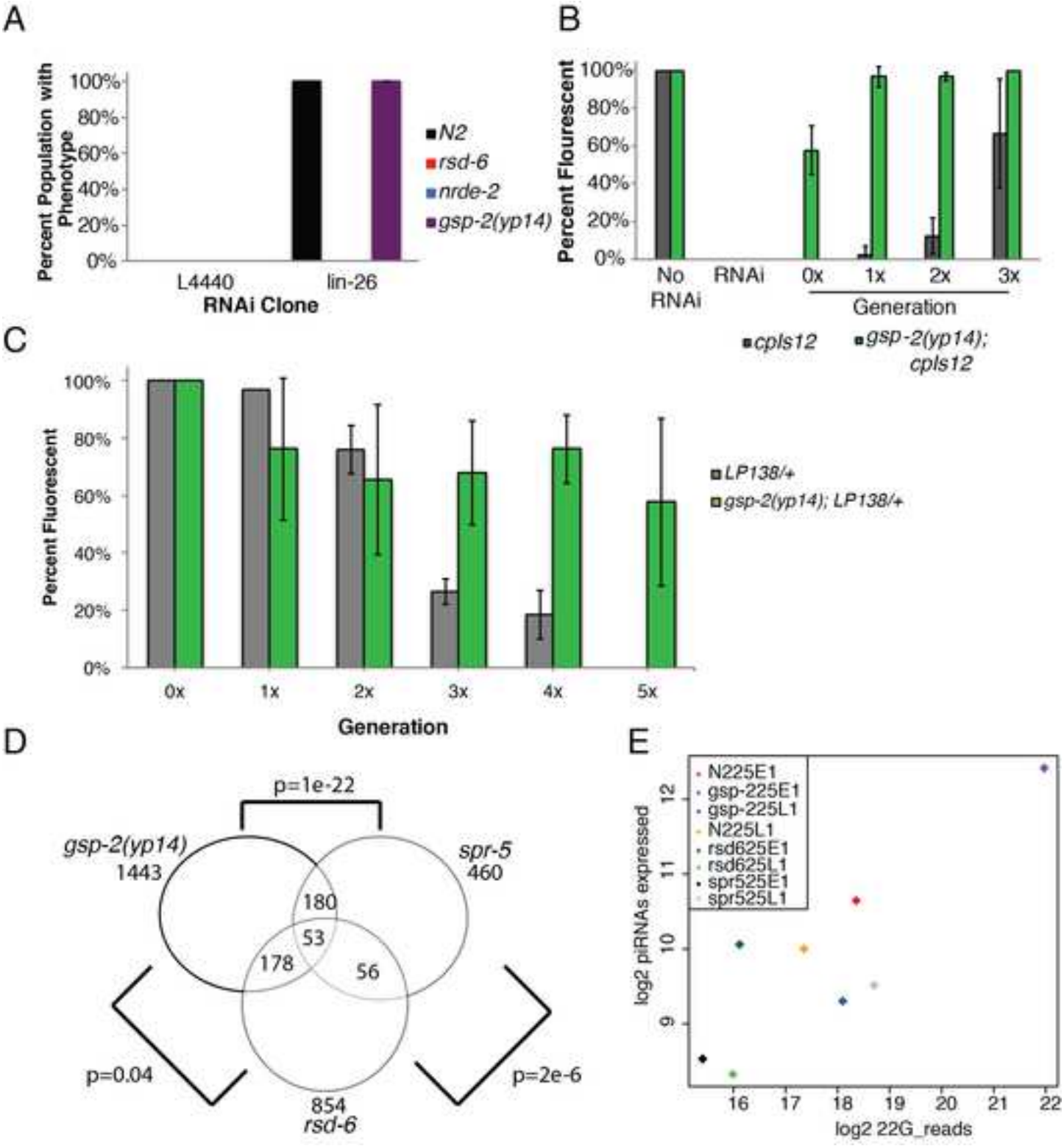

Figure 7